Potential of Carnot Batteries for load shifting of PV-production

Robin Tassenoy[a], Kenny Couvreur[a], Steven Lecompte[a,b] and Michel De Paepe[a,b]

[a] Department of Electromechanical,Systems and Metal engineering - Ghent University, Ghent, Belgium
[b] FlandersMake @ UGENT – Core lab EEDT – MP, www.flandersmake.be Leuven, Belgium
CA: robin.tassenoy@ugent.be

Abstract:

The share of renewable energy sources in our energy supply is ever increasing. Due to the intermittency of these renewable sources, large-scale electrical energy storage is needed to match supply and demand. Carnot batteries are a novel storage concept that could potentially fulfil this role. The needed system size for load-shifting of renewable energy sources is not well understood however. A high-level model for the primary sizing of a Carnot battery is presented to address this problem. The needed system size for load-shifting of solar PV-production in the Belgian grid is studied. The sensitivity of the size and performance of the total system to the performance of the different subsystems is investigated. Finally, the influence of variable electricity prices and non-ideal charging/discharging cycles on the levelized cost of storage (LCOS) is assessed by comparison to a previous study.

Keywords:

Carnot battery, load-shifting, large-scale electrical energy storage, integrating renewable energy sources, integrating solar PV-production

1. Introduction

The growth of renewable energy requires flexible, low-cost and efficient electrical storage to balance the mismatch between energy supply and demand. Pumped hydro storage, compressed air energy storage, flow batteries and electrochemical cells are the commercially available largescale energy storage technologies [1]. However, these technologies suffer from geographical constrains (such as pumped hydro storage and compressed air energy storage), require fossil fuel streams (like compressed air energy storage) or are characterized by a low cycle life (flow batteries and electrochemical cells). In mature electric grids, the easily exploitable additional capacity for pumped hydro energy storage is nearly exhausted [2]. For this reason, there is the need for new large-scale energy storage technologies, which do not suffer of the abovementioned drawbacks [3].

Carnot batteries are a novel storage concept that could potentially fulfil these needs. The storage concept involves three steps. First, electrical energy is converted into heat using a heat pump or joule heater. Secondly, the heat is stored. Finally, a heat engine technology is used to convert the heat back to electricity when needed. In the literature, different alternatives for the power-to-heat, thermal storage and heat-to-power systems have been considered. The charging and discharging power of the power-to-heat and heat-to-power system typically refer to the electrical input and output power respectively. The storage capacity of the system refers to the electrical storage capacity. This convention will be followed in this paper. If the thermal storage capacity of the thermal storage system is referred to, this will be stated explicitly.

In the most simple systems, an electric resistive heater is used for the power-to-heat conversion. The overall round-trip efficiency of these systems is severely affected by the low heat-to-power efficiency of the available heat engine technologies. Therefore, more complex power-to-heat systems are introduced based on heat pump technology. In this text, the terms power-to-heat system and heat pump (HP) will be used interchangeably. The terms heat-to-power system and heat engine (HE) will also be used equivalently. This paper focusses on heat pump based Carnot batteries. Examples of the most common topologies will be given. This selection is clearly not exhaustive, but is representative for the characteristics of the different types. For a more exhaustive discussion of the different system variants the reader is referred to the review paper of Dumont et al. [4]. Two main branches of heat pump based Carnot batteries exist: Brayton-based and Rankine-

based systems. Typically, the same cycle type is used for both the power-to-heat and heat-to-power conversion.

The Brayton-based systems can be divided in two main branches. The first branch has been introduced by Desrues et al. [5]. The system consists of two concrete regenerators, used as thermal storage and four turbomachines (one compressor/turbine pair used during the charging period and another pair during the discharging period). The turbomachinery is used to cycle gas (Argon) through the tank, following a closed thermodynamic Brayton-cycle. The maximum cycle temperature is 1000°C in the high temperature reservoir. A minimum temperature of -70°C occurs in the low temperature reservoir. A modest compression/expansion ratio of around 4.6 is used. The authors proposed a 100 MW/600MWh-system. A numerical analysis showed an estimated round-trip efficiency of 66.7% for a polytropic efficiency of the turbomachinery of 0.9. Mechanical and electrical losses were not included in this calculation however.

The second branch has been introduced by Howes et al. [6]. Again, the storage principle is based on a closed Brayton-cycle with Argon as working fluid, but volumetric machines are used. Only two volumetric machines are needed as they can operate in both compression and expansion mode. Two packed-bed thermal storage systems are used as hot and cold reservoirs. The nominal hot and cold temperatures are around 500°C and -150°C respectively. A higher pressure ratio of 10:1 is used compared to the system introduced by Desrues et al. [5]. The proposed system has been studied in more depth by White et al. [7] and McTigue et al. [8]. The latter found a round-trip efficiency of approximately 70% for a 2MW/16MWh-system using a polytropic efficiency of 0.99 for the compression and expansion devices. However, a round-trip efficiency of 46.4% has been found using a polytropic efficiency of 0.9. In contrast to the calculation done by Desrues et al., this analysis includes mechanical and electrical losses. If these losses are neglected, the round-trip efficiency of the thermodynamic cycle resulted in a value of 58%. The thermodynamic efficiency of both lay-outs is thus comparable.

Different Rankine-cycle based systems have been proposed too. Three main branches can be distinguished: subcritical systems based on steam-technology, subcritical systems based on ORC-technology and transcritical CO_2-cycles. The systems based on steam-technology have been introduced by Steinmann [9]. In a simplified thermodynamic analysis, a round-trip efficiency of 72.8% is found for a 1MW-system and an isentropic machine efficiency of 0.9 for the optimal multistage cycle-layout. The efficiency of the single stage systems without thermal integration reached an efficiency of 41.8%. For this simple lay-out, integration of a low temperature heat source is proposed to reach satisfying efficiencies. According to the author, the minimum power rating of the system should be around 5-10 MW to be economically feasible. Charging/discharging cycles of 6-10h are proposed. An example of a subcritical system based on ORC-technology is presented in Henchoz et al. [10]. The analysed system has a 50MW/400MWh-sizing. A cold storage at sub-ambient temperature levels is used as storage. The system is thermally integrated by solar collectors. These collectors are used to increase the temperature difference during the discharge and as such increase the system efficiency. The selected system has a round-trip efficiency of 57%, with an isentropic turbine efficiency of 0.9, a compressor efficiency of 0.88 and a pump efficiency of 0.85. Finally, transcritical Rankine-cycles have been introduced. Typically CO_2 is used as working fluid. A concept system of 50MW/100 MWh has been proposed by Morandin et al. [11]. A round-trip efficiency of 62% has been found with isentropic efficiencies ranging from 0.85 to 0.90.

The studies above all include a steady-state analysis and focus on the obtainable round-trip efficiencies of the system. The sizing of the system is chosen arbitrarily with electrical power outputs ranging from 1 MW to 100 MW and storage durations ranging from 2 to 8h. The choice for a specific power rating and charging/discharging duration is not elaborated upon. Moreover, the sensitivity of the system size to the performance of the subsystems is not studied in detail.

The IEA [12] estimated that the total wind and solar capacity will double on a worldwide scale between 2020 and 2025. Overall, renewables will account for 95 % of the increase in total power capacity through 2025. The European Commission [13] suggests a structural change in the process of power generation to RES to achieve 96 to 99 % decarbonization by 2050. At these increased levels of RES-integration load-shifting will be needed to store the excess electricity during peak production and to be able to use it during peak demand. However, the needed storage duration of the Carnot battery and power ratings of the subsystem's needed for this application have not been studied to the best of the author's knowledge. This study is a first attempt to size a Carnot battery for load-shifting of solar PV-production. A high-level model of a Carnot battery is used. The model is characterized by general performance parameters without any assumptions about the specific system lay-outs. Therefore, it can be used to study the influence of these parameters in general. It can be used to study a specific topology if the system characteristics are known. The sensitivity of the sizing and performance of the total system to the COP of the heat pump and the efficiency of the heat engine is considered. Finally,

the model is used to assess the influence of variable electricity prices and non-ideal charging and discharging cycles on the levelized cost of storage (LCOS) by comparison to a previous study.

2. Methodology

2.1. Input data

This study focusses on the use of a Carnot battery for load-shifting in an electrical grid with high integration of RES. Renewable sources are intermittent in nature. Therefore, moments of peak production do not correspond with periods of peak demand. A Carnot battery can be used to bridge this mismatch between supply and demand. An extreme case in which the total annual electricity production by solar PV is equal to the annual electricity demand is considered. In theory, an ideal storage thus can provide a perfect shift of the energy produced.

The electricity demand is simulated using a synthetic load profile for the year 2019 published by the system operator of the Belgian grid [14]. This is a dataset which represents the electricity consumption during each quarter hour of the year relative to the total annual consumption. It takes the yearly calendar (weekdays, weekends and holidays, time of sunrise and down, etc.) into account. In this study, an S21-profile is used to simulate the electricity demand of residential users. This profile is representative for residential users with a night-day-use-ratio smaller than 1.3. It is assumed that the renewable production capacity is intended to provide the electricity for residential users only.

The electricity production of the solar panels is simulated using a model developed by Laveyne et al. [15]. This model simulates the yield and production curve of decentralized solar panels placed in the low-voltage residential grid, depending on the panel orientation and the irradiation data. In the study, irradiation data representative for Belgium is used. A novel ”all-sky distribution” model is used to take the contribution of diffuse irradiation on the PV-panel into account. This model is suitable for the Belgium irradiation profile. Based on the total irradiance, the power output of a typical solar PV-panel is calculated. Finally, an inverter model is taken into account. This results in the useful AC-production of the solar panels. The most optimal orientation given the Belgian irradiation data is assumed, which corresponds with an azimuth of 0 degrees and a tilt angle of 34.5 degrees.

The synthetic load profile and the normalized solar PV electricity production for one year are shown in Figure 1 (a). In these normalized profiles, the energy fraction of each quarter of an hour relative to the total annual energy production and demand is tabulated. The summation of all energy fractions over the year thus equals 1 for both the production and demand profile. In Figure 1 (b), a more detailed view of the profiles in one summer week is shown. It can be seen that the fluctuation in solar PV production is higher than the fluctuation in demand. The solar PV production shows a daily cycle. At night, the production drops to zero, while the production peaks at noon. Even during this peak the production shows significant fluctuation due to fluctuation of the irradiation of the panels. The fluctuations in the residential demand are smaller. The electricity demand is the highest in the winter and the lowest during the summer. As visible in Figure 1 (b), the energy demand is slightly lower on weekdays than during the weekend (days 186 and 187). The dip between the morning and evening peak in the electricity demand is smaller during the weekends. It is important to note however that these profiles are representative for a time period before the COVID-pandemic. Due to the pandemic, a lot of people work from home which is likely to affect the residential energy demand.

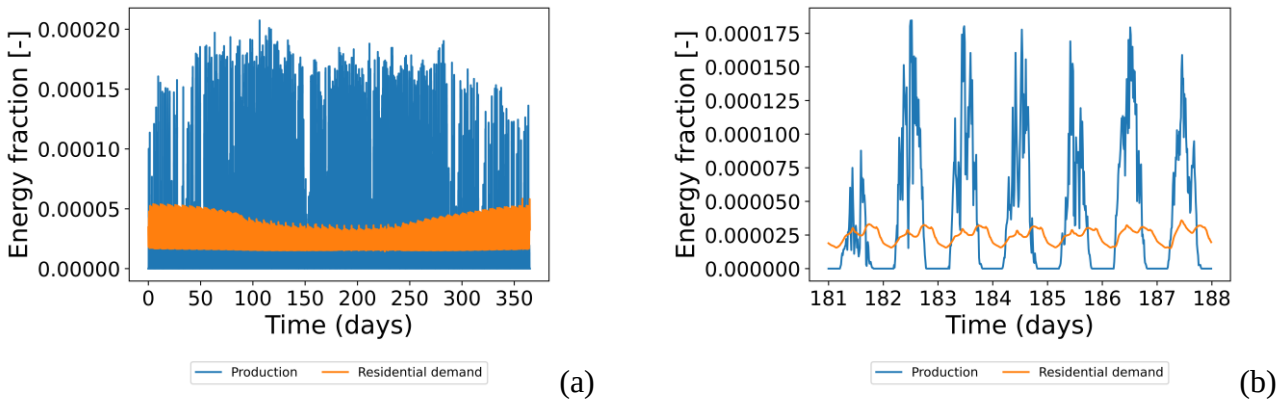

Figure 1: normalized production and demand profile for one year (a) and one summer week (b)

The normalized profiles are scaled with the yearly electricity consumption of a potential use case. The average electricity consumption of a Belgian family equalled 3025 kWh/year in 2019 [16]. In the current study, the total electricity consumption of 120 000 families is considered. This corresponds roughly with the number of households in Ghent, Belgium. As explained before, an extreme case in which this total yearly electricity demand is produced entirely by solar PV is considered. A perfect shift of the overproduction is thus possible in case the round-trip efficiency of the storage equals 1. To synchronize supply and demand, a total of 230743.6 MWh of electrical energy should be shifted over the course of one year. When discussing the amount of energy charged and discharged by the Carnot battery, this will be expressed relative to this maximal needed shift. As such, the service delivered by the system can be interpreted more easily. The minimum and maximum power ratings during one quarter of the year are summarized in Table 1.

Table 1: Maximum and minimum power for the production and demand profiles

Use case	Maximum power [MW]	Minimum power [MW]
Production	301.1	0.0
Residential demand	84.8	20.8

To make a first estimate of the financial aspects, electricity prices of the Belgian day-ahead market in 2019 were used [17]. These prices correspond with the demand profiles used.

2.2. System model

A high-level model of a Carnot battery is considered. The system consists out of three building blocks: the power-to-heat system, the thermal storage system and the heat-to-power system. Each block is characterized by general performance parameters, as illustrated in Figure 2.

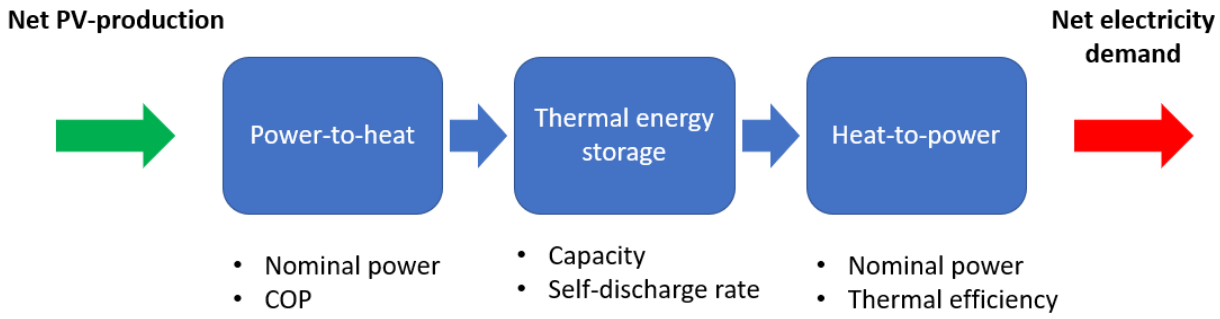

Figure 2: Overview of the high-level system model of a Carnot battery and the general performance parameters of the subsystems.

The power-to-heat system is characterized by its power rating (MW) and its coefficient of performance (COP). A COP equal to one corresponds with an electrical joule heater, while a higher COP could be obtained with a heat pump. The heat-to-power system is characterized by its power rating (MW) and its thermal efficiency. The thermal storage system is characterized by its thermal storage capacity (MWh_{th}) and its self-discharge rate. The TES-capacity is expressed as a charging/discharging-duration at full power. The needed TES-capacity (MWh_{th}) for a storage duration is calculated based on both the nominal power of the heat pump (taking the COP into account) and heat engine (taking the efficiency into account). The largest value is taken for the absolute capacity of the storage. The self-discharge rate is expressed as a percentual heat loss of the current state-of-charge per quarter of an hour.

Remark that the goal is not to make a detailed system model, but rather to get a first impression of the influence of the variable production and demand profiles and of the performance characteristics of the subsystems on sizing of the complete system. As no assumptions on the actual system lay-outs (used cycles, storage temperatures,. . .) are made, dynamic and part-load system characteristics are not included in the current model. Performance of the components is assumed constant and an immediate response of the system in each time step is used.

2.3. Charging/discharging-decision algorithm

The system's operation strategy aims at integrating as much as possible RES-electricity into the grid.

First, the difference between the production and the demand is calculated for each quarter of an hour of the year. If this net production is positive, this excess electricity production will be used to charge the system. If the net production is negative, thermal energy will be extracted from the TES and electricity will be produced by the heat engine. The maximum and minimum net production power is shown in Table 2.

The heat pump power is expressed relative to the maximum power. The electrical power of the heat engine is expressed relative to the absolute value of the minimum power. For a chosen system size the charging and discharging behaviour is calculated. From this behaviour the optimal system size is selected following the strategy discussed in Section 2.6.

Table 2: Maximum and minimum net production power for residential demand

Use case	Maximum power [MW]	Minimum power [MW]
Residential demand	257.7	-84.8

During charging, the net production power is compared to the maximum power of the heat pump. If the net production power is higher or equal to this maximum power, the system will run at maximum power. If not, the system power is set equal to the available excess power. Part-load behaviour is not considered and the COP is thus assumed constant. Once the charging power is determined, it is verified the free capacity of the TES is sufficient to store the heat corresponding with charging one quarter of an hour at this power. If not, the heat pump power is lowered so that the TES is completely charged at the end of the timestep. During discharge a similar procedure is used. First, the net production power is compared to the maximum heat engine power. Depending on this comparison, the heat engine will function at full or part load. The heat engine efficiency is assumed constant. If the thermal energy in the TES is not sufficient to run the heat engine at this power, the discharge power is reduced and the TES will be completely discharged at the end of the timestep.

2.4. Performance evaluation

To evaluate the system's performance following parameters are of main interest: the fraction of the total overproduction of electricity stored over one year, the fraction of the total underproduction delivered by the Carnot battery and the system's round-trip-efficiency. The round-trip efficiency can be calculated as [4]:

$$\eta_{RT,th} = COP_{HP} * \eta_{TES} * \eta_{HE} \quad (1)$$

2.5. Subsystem performance: base case and sensitivity ranges

To illustrate the use of the high-level model for sizing of the Carnot battery a baseline configuration is defined first. To get generally representative results, this baseline should be representative for the different system topologies. To get a first impression of the expected system's round-trip efficiency, the mean efficiency of the different studies discussed in section 1 can be considered. The average round-trip efficiency found equals 61.8%.

In the current model, the round-trip efficiency of the overall system is retrieved by defining suitable efficiencies of the subsystems. To get reasonable estimates, following values have been found in literature.

The COP of the power-to-heat system is often not mentioned separately. Steinmann [9] made a summary of the parameters of the heat engines applied in Carnot batteries. The cycle-efficiencies of these heat engines is combined with the overall round-trip efficiency of a Brayton-based Carnot battery determined by McTigue et al. [8] to make an estimation of the COP of the heat pump. The COP of a Brayton-based heat pump is estimated as 3.8. To get an impression of the COP of Rankine-based systems, a review by Arpagaus et al. [18] is referred to. The authors made an overview of the current state-of-the-art of large-scale high temperature, Rankine-based heat pumps with heat sink temperatures in the range of 90-160°C. The COP-values found range from 2.4 to 5.8 depending on the model and operational conditions. A mean COP-value of 3.3 has been found. The self-discharge of the TES is often neglected. According to McTigue et al. [8] these heat losses can be reduced to any desired level with sufficient insulation. White et al. [7] suggested that a 1% daily heat leakage from or to each reservoir in the studied Brayton-based system would reduce the round-trip efficiency by about 2%. These losses are expected to be even smaller for other topologies, as the Brayton-based systems typically are associated with the highest temperatures for the hot storage and the lowest temperatures for the cold

storage. Steinmann [9] composed a summary of the efficiencies of the different thermal cycles considered for the discharge process of a Carnot battery. Depending on the pressures and maximum temperatures considered, the cycle efficiencies found range from 9.6% for a Brayton-based heat engine at limited temperatures to 41.8% for a Rankine-based heat engine at high temperature (for this type of cycle). A more elaborate review of efficiencies of ORCs in different applications and thus expected temperature ranges is given by Li et al. [19]. The efficiencies found range from 6.84% to 26.9%.

Based on the considerations above, the base case is defined as shown in Table 3. The ranges for the performance of the different subsystems to study the sensitivity of the results are indicated in the same table.

Table 3: Overview subsystem performance base case and ranges sensitivity study

Performance parameter	Base case	Sensitivity range
COP_{HP}	3	1 – 6
η_{TES}	1	/
η_{HE}	0.2	0.05 – 0.40

2.6. Sizing strategy

To evaluate the sizing of the base case system, a gradual approach is used. First, the needed TES-duration is studied assuming the system's charging and discharging is never limited by the power rating of the thermal machines. The power of both the heat pump and the heat engine is set equal to the maximum value of the net production and demand over the year. For the studied profiles, this results in a heat pump power to heat engine power ratio of 3. The performance of the system in function of the TES-duration has been discussed. For the optimal duration, the power of the heat pump and heat engine have been varied to study potential size reduction and their impact on the system performance. Finally, the optimal size for the current case is selected. The results of this sizing procedure are summarized in Section 3.1.

2.7. Sensitivity analysis

The sensitivity of the optimal size is considered by varying the system performance parameters of the heat pump and the heat engine. In this analysis, the nominal power of the thermal machines and the TES-storage duration have been kept constant. The results are discussed in Section 3.2.

2.8. Financial analysis

To assess the economic competitivity of the system, the levelized cost of storage (LCOS) is calculated. To this purpose, CAPEX-estimates by Smallbone et al. [20] are used. These estimates are constructed based on a Brayton-based topology. The results are thus no longer generally applicable but only valid for the specific type of system described in that paper. Nevertheless, the same CAPEX-estimates have been used to assess the economic competitivity of Rankine-based systems as well [21]. The LCOS is calculated as:

$$LCOS = \frac{CAPEX + \sum_{t=1}^{t=n} \frac{A_t}{(1+i)^t}}{\sum_{t=1}^{t=n} \frac{W_{out}}{(1+i)^t}} \quad (2)$$

$$A_t = OPEX_t + CAPEX_{re,t} + c_{el} W_{in} - R_t \quad (3)$$

In which CAPEX represents the systems investment cost, A_t represents the annual system costs, $c_{el} W_{in}$ the total charging cost, R_t the recovery value of system components with a longer lifetime and W_{out} the total electrical energy discharged by the system over one year.

Smallbone et al. [20] determined the LCOS for a Brayton-based demonstrator plant for a system with 2MW charging power, 16 MWh storage capacity and 1.6 MW discharge power. They distinguished three different scenarios: the technology potential, the target system and the conservative estimate. The systems roundtrip efficiency ranges from 72% to 52% depending on the case. The authors made different estimates of the CAPEX and OPEX of the system for each scenario. The energy based CAPEX is expressed per amount of electrical energy stored. The corresponding thermal storage capacity of the TES (MWh_{th}) depends on the round-trip efficiency of the system. Therefore, only the conservative scenario will be used for comparison in this study. The parameters used by Smallbone et al. are summarized in Table 4.

Table 4: Summary of conservative scenario studied by Smallbone et al. [20]

	Units	Conservative estimates
Roundtrip efficiency	%	52
Self-discharge rate (loss of energy in storage)	% per day	1
System lifetimes	years	20
Specific CAPEX power based	EUR/kW	797
Specific CAPEX energy based	EUR/kWh	21
Specific OPEX power based	EUR/kW	0.0026
Specific OPEX energy based	EUR/kWh	11
Insurance rate	%	0.5
Discount rate	%	8
Input/output power ratio	kW/kW	1.25

The main difference between previous studies and the current analysis is twofold. Firstly, fluctuating electricity pricing date from the Belgian day-ahead market is used where others used a fixed electricity price to calculate the charging cost. Secondly, the charging/discharging is based on representative production and demand profiles suitable for the application of interest. The charging/discharging-cycle is thus no longer a perfect repetition of a daily cycle with a complete system charging during 8h and a complete system discharge during 10h. Charging/discharging is dependent on the production and demand profiles used according to the operation strategy described in Section 2.3.

The performance of the subsystems separately is not described by Smallbone et al. [20]. In line with the findings of Section 2.5 and the round-trip efficiency used by Smallbone et al. , the subsystem parameters are chosen as indicated in Table 5.

Table 5: subsystem performance for financial analysis

COP_{HP}	η_{TES}	η_{HE}
3.8	1	0.137

The goal of this paper is not to provide a detailed financial analysis of the Carnot battery technology (as this requires specific knowledge of the detailed system topology), but rather to illustrate the influence of variable electricity pricing and non-ideal charging and discharging cycles on the LCOS.

3. Results

In this section, the simulation results are discussed. First, the sizing of the system is treated. Secondly, the sensitivity of the sizing to the performance of the subsystems is considered. Finally, the LCOS-calculation is discussed.

3.1. Base case sizing

In Figure 3, the relative energy charged and discharged by the base case system are shown as function of the available TES-storage duration. This illustrates the fraction of the overproduction and underproduction that is charged and discharged by the system over the year. TES-storage durations ranging from 1 to 24h have been considered. Additional TES-storage duration initially increases the amount of energy charged significantly. Typically, several hours of overproduction are present during day-light hours. This overproduction cannot be recovered optimally if the TES-storage duration is too small. At a certain point, the additional benefit of added storage drops. In practise, the supplementary service should be weighted to the additional investment cost of the system. Depending on the desired amount of service, a storage duration of 6-10h has been found to be optimal. A storage duration of 8h has been selected for further study.

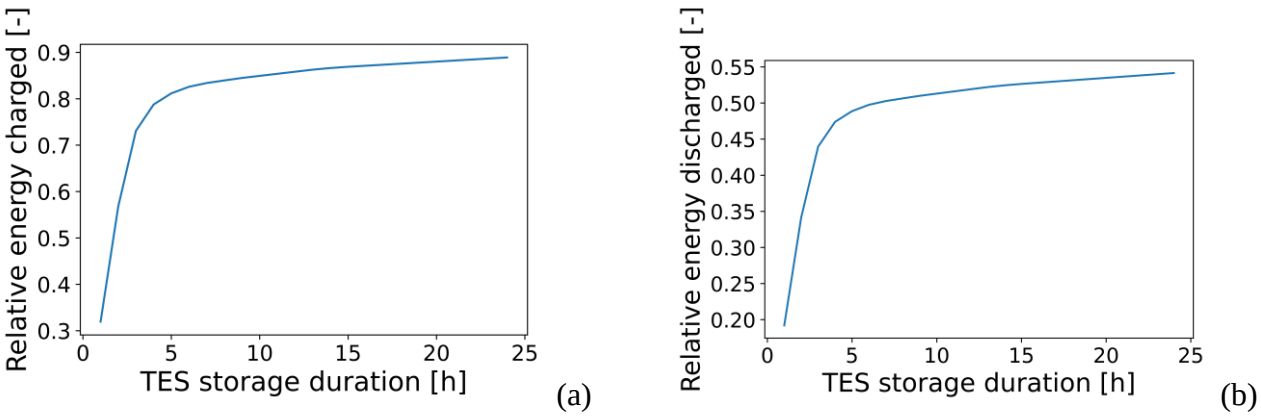

Figure 3: relative energy charged (a) and discharged (b) as function of the TES storage duration for the base system without power limitations ($COP_{HP} = 3, \eta_{TES} = 1,\ \eta_{HE} = 0.2, P_{HP,rel} = 1, P_{HE,rel} = 1$)

For this base system with a TES-storage duration of 8h, the relative heat pump and heat engine power have been varied. Only the size of the subsystems has been changed. The performance parameters have been kept constant. The round-trip efficiency of all systems considered is thus equal to 0.6. From Figure 4, it becomes clear the power of the thermal machinery can be reduced significantly for a limited drop in service delivered. The drop in performance is more sensitive to a drop in heat pump power compared to a drop in heat engine power. This is illustrated in Table 6. When the power of both thermal machines is halved, the relative energy discharged by the system drops only 6.3%. It is important to note that the absolute TES-capacity (MWh_{th}) is also divided by two to reach the same TES-storage duration of 8h. Using the CAPEX-estimates described in Table 4, the CAPEX of the system is thus halved too.

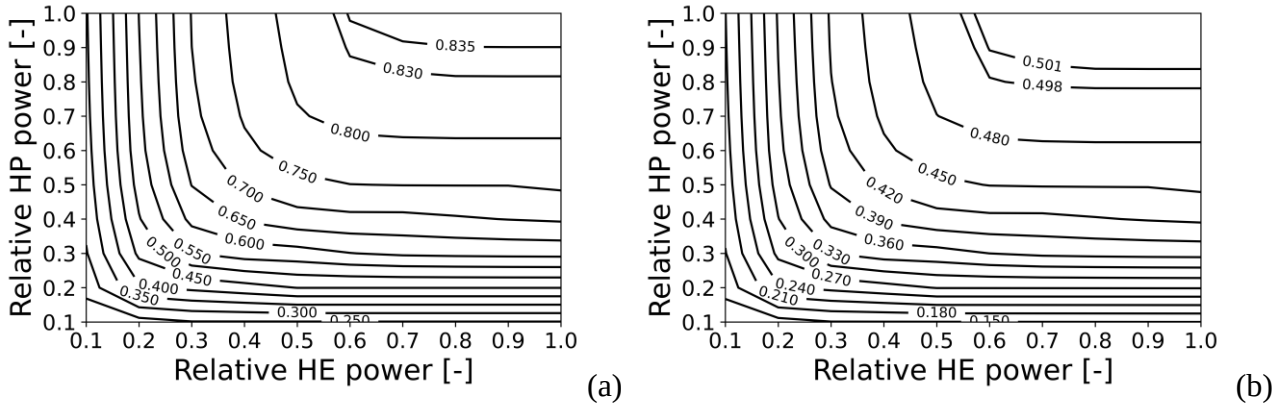

Figure 4: relative energy charged (a) and discharged (b) as function of the relative heat pump and heat engine power for the base system ($COP_{HP} = 3, \eta_{TES} = 1,\ \eta_{HE} = 0.2$) with a TES-storage duration of 8h

Table 6: relative energy charged and discharged for the base system ($COP_{HP} = 3, \eta_{TES} = 1,\ \eta_{HE} = 0.2$) with a TES-storage duration of 8h for a selection of relative heat pump and heat engine powers

Relative HP power [-]	Relative HE power [-]	Relative energy charged [-]	Relative energy discharged [-]
1	1	0.839	0.506
0.5	1	0.756	0.457
1	0.5	0.817	0.493
0.5	0.5	0.737	0.443

3.2. Sensitivity to subsystem performance

In Figure 5 (a) and (b), it can be seen that the amount of energy charged and discharged depends on the round-trip efficiency, when the power of the thermal machines is fixed and the storage duration is constant. As illustrated by Figure 5 (c), systems with the same round-trip efficiency deliver the same service. However, the needed absolute TES-capacity (MWh_{th}) to reach the same TES-storage duration differs depending on how this round-trip efficiency is obtained. A higher HP COP and lower HE efficiency require a higher absolute TES-capacity (MWh_{th}) to reach the same TES-storage duration. When different round-trip efficiencies are considered, it can be seen that the lower the system's round-trip efficiency the higher the relative energy charged by the system. Due to the lower round-trip efficiency the energy delivered by the system is still lower however. For systems with a higher round-trip efficiency the amount of electricity used for charging the system drops, while the amount discharged rises. This means a smaller share of the overproduced RES-electricity is recovered and it could be beneficial to increase the system size. It is important to note that these higher round-trip efficiencies can only be obtained by thermally integrated systems. The theoretical maximum obtainable round-trip efficiency without thermal integration is 1. All systems with a higher round-trip efficiency can thus not operate between the same two thermal reservoirs. The heat source should have a higher temperature than the heat sink. These systems thus require an additional energy input under the form of heat at a higher temperature. The zone indicated in red on Figure 5 can thus only be reached if a sufficiently large residual heat source at a sufficiently high temperature is present. In practise, the zone that requires thermal integration will be larger than the zone indicated here due to irreversibilities. The needed additional energy input is related to the system size and should thus be taken into account during sizing of the system.

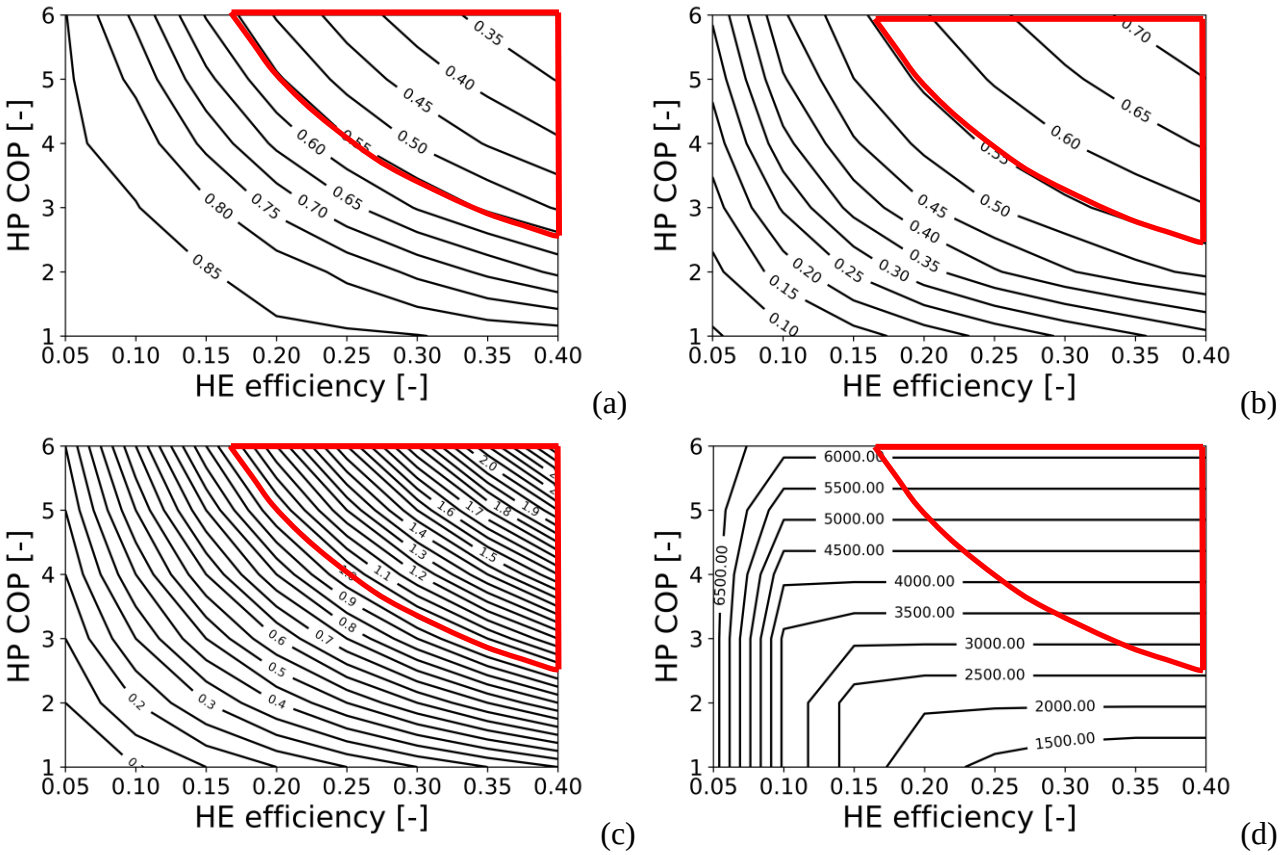

Figure 5: Influence of variable HP COP and HE efficiency for a fixed system size ($\eta_{TES} = 1$, $P_{HP,rel} = 0.5$, $P_{HE,rel} = 0.5$, $TES_{duration} = 8h$) (a): relative energy charged (b): relative energy discharged (c): round-trip efficiency (d): TES-capacity (MWh_{th}). The zone indicated in red can be reached with thermally integrated systems only.

3.3. Financial analysis

As explained in Section 2.8, the results in this section are no longer applicable for a general system, but focus on the Carnot battery topology described by Smallbone et al. [20]. They found a LCOS of 110 EUR/MWh for a small 2MW/16MWh-system. As explained before, the current study differs by the use of variable electricity pricing and the charging/discharging strategy used. A LCOS of 153.7 EUR/MWh has been found for the

2MW/16MWh-system. The variable pricing and non-ideal charging and discharging cycles thus have a significant effect on the LCOS.

It is important to note that the 2MW/16MWh-system is quite small compared to the RES-production studied. This system thus has a low relative energy charged and discharged. For larger systems, the LCOS is even higher. If the goal of the system is to integrate more RES into the grid, the system size should be large enough to make a significant contribution. At these larger sizes, the charging/discharging cycle is not fully used and the number of cycles over the year is limited by the available net electricity production. Therefore, the increase in CAPEX of the system and the additional charging costs cannot be compensated by the additional amount of energy discharged. An important side note is that the used pricing data corresponds with an electrical grid where the RES-penetration is not very high. It is possible that massive RES-integration will cause changes into the electricity price fluctuations. When calculating the LCOS, it is thus interesting to take the system size and operation strategy, intended use case and variable electricity prices of the intended market into account.

4. Conclusion

A first discussion of the sizing of a Carnot battery for shifting PV-production for residential use has been made. A general high-level model of a Carnot battery has been used.

A base case system with $COP_{HP} = 3, \eta_{TES} = 1,\ \eta_{HE} = 0.2$ has been defined. For this system, a TES-storage duration of 6-10h has been found suitable for load-shifting of solar PV-production. It has been found that the power of the heat pump and heat engine can be reduced significantly for a limited reduction in service over the year. The service delivered is more sensitive to the relative heat pump power than to the relative heat engine power. The sensitivity of the sizing to the performance of the subsystems has been evaluated. The optimal component sizes depend on the round-trip efficiency of the system. Systems with the same round-trip efficiency result in the same service delivered by the system for a given power of the thermal machines and TES-storage duration. For a given round-trip efficiency, it is beneficial to maximize the heat engine efficiency while keeping the heat pump COP small. This minimizes the absolute TES-capacity needed for the desired TES-storage duration.

The influence of variable electricity pricing and non-ideal charging/discharging cycles on the LCOS of the system has been studied by comparison to a previous study. The LCOS calculated in this dynamic setting is significantly higher.

From this study the importance of taking the dynamic nature of production and demand data and electricity pricing during the study of these systems is illustrated. As a general model is used, part-load behaviour has been neglected and constant performance of the subsystems has been assumed. In future work, the dynamic characteristics and part-load behaviour of different system topologies will be assessed in detail. The impact of these characteristics on the results obtained here will be evaluated.

References

[1] European Commission. Clean energy for all Europeans 2016.

[2] Gimeno-Gutiérrez M., Lacal-Arántegui R., Assessment of the European potential for pumped hydropower energy storage based on two existing reservoirs. Renewable Energy 2015;75:856–68.

[3] Argyrou M.C., Christodoulides P., Kalogirou S.A., Energy storage for electricity generation and related processes: Technologies appraisal and grid scale applications. Renewable and Sustaintainable Energy Reviews 2018;94:804–21.

[4] Dumont O., Frate G.F., Pillai A., Lecompte S., De Paepe M., Lemort V., Carnot battery technology: A state-of-the-art review. Journal of Energy Storage 2020; 32: 101756

[5] Desrues T., Ruer J., Marty P., Fourmigué J.F., A thermal energy storage process for large scale electric applications. Applied Thermal Engineering 2010;30(5):425-32

[6] Howes J., Concept and Development of a Pumped Heat Electricity Storage Device. Proceedings of the IEEE 2012; 100(2):0019-9219

[7] White A., Parks G., Markides C.N., Thermodynamic analysis of pumped thermal energy storage. Applied Thermal Engineering 2013;53(2):291-98

[8] McTigue J.D., White A., Markides C.N., Parametric studies and opimisation of pumped thermal electricity storage. Applied Energy 2015;137:800-11

[9] Steinmann W.D., The CHEST (Compressed Heat Energy Storage) concept for facility scale thermo mechanical energy storage. Energy 2014; 69: 546-52

[10] Henchoz S., Buchter F., Favrat D., Morandin M., Mercangöz M., Thermoeconomic analysis of a solar enhanced energy storage concept based on thermodynamic cycles. Energy 2012;45:358-65

[11] Morandin M., Mercangöz M., Hemrle J., Maréchal F., Thermoeconomic design optimization of a thermo-electric energy storage system based on transcritical CO_2 cycles. Energy 2013; 58: 571-87

[12] International Energy Agency (IEA), Renewables 2020 Analysis and forecast to 2025 – Available at: <https://www.iea.org/reports/renewables-2020 > [accessed 24.03.2021]

[13] European Commission, 2011, Energy Roadmap 2050.

[14] Vlaamse Regulator van de Elektriciteits- en Gasmarkt. VREG Synthetic Load Profiles – Available at: <https://www.vreg.be/nl/verbruiksprofielen> [accessed 19.02.2021]

[15] Laveyne J. Bozalakov D., Van Eetvelde G., Vandevelde L., Impact of Solar Panel Orientation on the Integration of Solar Energy in Low-Voltage Distribution Grids. International Journal of Photoenergy 2020; Volume 2020: Article ID 2412780

[16] Vlaamse Regulator van de Elektriciteits- en Gasmarkt. VREG Evolution energy consumption – Available at: <https://www.vreg.be/nl/evolutie-energieverbruik#1> [accessed 19.02.2021]

[17] European Network of Transmission System Operators for Electricity (ENTSO-E). ENTSO-E Transparancy Platform – Available at:<https://transparency.entsoe.eu/transmission-domain/r2/dayAheadPrices/show> [accessed 11.02.2021]

[18] Arpagaus C., Bless F., Uhlmann M., Schiffmann J., High temperature heat pumps: Market overview, state of the art, research status, refrigerants, and application potentials. Energy 2018; 152: 985-1010

[19] Li G., Organic Rankine cycle performance evaluation and thermoeconomic assessment with various applications part I: Energy and exergy performance evaluation. Renewable and Sustainable Energy Reviews 2016; 53: 477-99

[20] Smallbone A., Jülch V., Wardle R., Roskilly A. P., Levelised Cost of Storage for Pumped Heat Energy Storage in comparison with other energy storage technologies. Energy Conversion and Management 2017;152:221-28

[21] Dumont O., Lemort V., Mapping of performance of pumped thermal energy storage (Carnot battery) using waste heat recovery. Energy 2020; 211: 118963